

Abstract

Integrated distribution models (IDMs), in which datasets with different properties are analysed together, are becoming widely used to model species distributions and abundance in space and time. To date, the IDM literature has focused on technical and statistical issues, such as the precision of parameter estimates and mitigation of biases arising from unstructured data sources. However, IDMs have an unrealised potential to estimate ecological properties that could not be derived from the source datasets if analysed separately. We present a model that estimates community alpha diversity metrics by integrating one species-level dataset of presence-absence records with a co-located dataset of group-level counts (i.e. lacking information about species identity). We illustrate the ability of IDMs to capture the true community alpha diversity through simulation studies and apply the model to data from the UK Pollinator Monitoring Scheme, to describe spatial variation in the diversity of solitary bees, bumblebees and hoverflies. The simulation and case studies showed that the proposed IDM produced more precise estimates of the community diversity than the single models, and the analysis of the real dataset further showed that the alpha diversity estimates from the IDM were averages of the single models. Our findings also revealed that IDMs had a higher prediction accuracy for all the insect groups in most cases, with this performance linked to the information provided by a data source into the IDM.

Key words: Alpha diversity, Bayesian models, Markov Chain Monte Carlo methods, Multispecies distribution models, UK Pollinator Monitoring scheme

1 Introduction

Biodiversity monitoring programs generate disparate data types that are used to infer and make predictions about species distributions, dynamics and diversity (Kéry and Royle, 2015, 2020; Isaac et al., 2020; Bird et al., 2014). From the various datasets available, there is now a plethora of modelling approaches to deal with various aspects of the ecological and observational processes in response to the availability of large and varied data from different sources and survey and sampling protocols. The vast majority of these modelling approaches were developed with one particular data type in mind, such as count data or presence-only records. In recent years, the growing heterogeneity of data types has made integrated distribution models (IDMs) an emerging development in ecological statistics and species distribution modelling (Pacifci et al., 2017; Koshkina et al., 2017; Miller et al., 2019; Isaac et al., 2020). IDMs involve integrating datasets of different

29 types into one model that explicitly captures the features of each.

30 There are different approaches to developing an integrated model. One data set can be used as a fixed
31 effect to model the other (covariate structure), or datasets can share information through their correlation in
32 space and possibly time (correlation structure; Pacifici et al., 2017; Miller et al., 2019). The most common
33 implementation of IDMs uses a joint likelihood in a hierarchical Bayesian framework (Miller et al., 2019).
34 In the joint likelihood framework, each dataset is conceptualised as an independent realisation of the same
35 underlying ecological state variables (e.g. abundance or occupancy). The strength of the joint likelihood
36 approach comes from sharing information between datasets through common parameters and/or by sampling
37 the same locations in multiple datasets.

38 Most studies on IDMs are either case studies of particular applications (Doser et al., 2022) or explorations
39 of statistical challenges that data integration brings (Simmonds et al., 2020; Ahmad Suhaimi et al., 2021).
40 Typically, these have addressed the degree to which spatial biases in unstructured data can be overcome, and
41 the precision of the parameters being estimated (Simmonds et al., 2020; Ahmad Suhaimi et al., 2021; Koshkina
42 et al., 2017). These studies have shown, either by using the model predictive accuracy and/or the accuracy and
43 precision of estimated parameters, that IDMs can, in some circumstances, perform better than single models or
44 models developed from a subset of all the datasets (Koshkina et al., 2017; Pacifici et al., 2017; Miller et al.,
45 2019; Isaac et al., 2020; Simmonds et al., 2020; Zulian et al., 2021).

46 An unrealised benefit of IDMs is the potential to estimate parameters that would not be estimable from
47 either of the data sets if analysed separately. Usually, community alpha diversity measures such as Shannon and
48 Simpson indices are estimated using abundance-based diversity metrics and these indices need species-level
49 abundance information (Hill, 1973; Gatti et al., 2020). However, it is not always possible to identify individuals
50 to their species level. This is often true for insect monitoring, where counts may be resolved to a coarser
51 taxonomic level. This can arise for a number of reasons, such as: the cryptic nature of some species (requiring
52 microscopic examination to separate similar species), the need for specialised taxonomy skills and organisms
53 being observed only briefly (e.g. on the wing).

54 The vast majority of biodiversity data available, such as presence-absence, capture-recapture, and presence-
55 only data, do not contain information on abundance but may have information on the species identity. Alpha
56 diversity indices can be estimated from the presence-absence data when imperfect detection has been accounted
57 for in a multi-species occupancy model, as has been done in some studies (Gotelli and Chao, 2013; Broms

58 et al., 2015; Guillerá-Arroita et al., 2019). These species-level presence-absence data, however, are less
59 informative than count data (Broms et al., 2015), and the diversity indices estimated can be strongly affected
60 by the model structure such as parametric assumptions, prior specifications and prior choices (Guillerá-Arroita
61 et al., 2019).

62 In this study, we combine these two data types in an IDM to estimate community alpha diversity parameters
63 that could not be "properly" estimated from the datasets when analysed separately. To date, no studies we
64 are aware of have attempted to demonstrate this potential from IDMs, but it is something that integrated
65 population models (IPMs) have been used for for a long time (Besbeas et al., 2002; Abadi et al., 2010; Schaub
66 et al., 2007). For example, Besbeas et al. (2002) integrated census data (providing information about the total
67 number of organisms) and ring recovery data (providing information on individual organisms) to estimate
68 birth, death and fecundity at the population level.

69 Our model is parameterised using data from the UK Pollinator Monitoring Scheme (PoMS) (O'Connor
70 et al., 2019; Breeze et al., 2021), which has been generating monitoring data on pollinating insects in the UK
71 for the last five years and is now informing an EU-wide pollinator monitoring scheme (Potts et al., 2020).
72 PoMS collects two types of data: one dataset contains presence-absence data on individual species (using pan
73 traps), and the other contains counts that are not resolved to the species level (so-called Flower-Insect Timed
74 Counts or "FIT Counts"). Our analyses of PoMS data are supported by simulations. We demonstrate that
75 between them, these datasets can provide inferences about site-level alpha diversity that would not be possible
76 using either dataset in isolation. The model developed here will be useful in situations where professional and
77 mass participation schemes collect data on the same organisms and where the species are difficult to identify
78 (e.g. most insect groups).

79 **2 Methods**

80 We first provide a motivation for the methods of this study by exploring the PoMS data. We then describe
81 the overall structure of the data. We define the state models representing each species' unknown site-specific
82 abundance and occupancy. The state variables are defined in terms of spatial point processes, which provide
83 a flexible way to integrate datasets in different ecological currencies (Miller et al., 2019; Isaac et al., 2020).
84 We then define sub-models for each of the two data types. The final two sections of the Methods deal with

85 inference and the estimation of community parameters.

86 **2.1 UK Pollinator Monitoring Scheme Data**

87 The data used is a subset of the PoMS data (Breeze et al., 2021; O'Connor et al., 2019; Scheme, 2022a,b).
88 PoMS implements a systematic survey with 95 1 km square sites selected following a stratified sampling
89 design across Great Britain (GB) and Northern Ireland (NI). The sites are surveyed up to four times per year
90 from May to September, with a minimum of two weeks between each consecutive survey at a site. On the
91 same visit, the observer implements two survey protocols: a pan trap survey and a FIT count survey (Breeze
92 et al., 2021; O'Connor et al., 2019). On each visit, five pan trap stations (each hosting three coloured bowls
93 painted UV-bright yellow, blue and white, mounted at vegetation height and filled with water) are set out
94 along a diagonal of each 1 km square site and left for six hours. During this time, the surveyor undertakes at
95 least two ten-minute FIT counts, which involves counting all insects landing on a target flower in a 50x50
96 cm patch. Pollinators are identified at the level of a broad taxonomic group, e.g. bumblebees, solitary bees,
97 and hoverflies. After six hours, the samples from the pan traps are collected and sent to a lab for professional
98 identification. Therefore, each visit to the 1km site produces a list of bee and hoverfly species found in the pan
99 traps and group-level count data from the FIT counts. The data used in this study were from the first two years
100 (2017 - 2018) of PoMS, during which 74 of the 75 survey sites across GB returned suitable data (PoMS was
101 not active in NI in the first two years). The summary of the group-level count data and species occupancy data
102 are presented in Table 1 and the distribution of each dataset at each study site is provided in Supplementary
103 information 1 Figures S1-1 to S1-6.

| Insect group | FIT counts | Pantrap occupancy | |
|---------------|--------------|-------------------|----------------------|
| | Average (SD) | $N_{species}$ | Naive occupancy (SD) |
| Bumblebees | 1.11 (5.18) | 17 | 0.086 (0.20) |
| Hoverflies | 2.74 (10.92) | 79 | 0.055 (0.01) |
| Solitary bees | 0.29 (1.62) | 70 | 0.027 (0.111) |

Table 1: Summaries of the group-level FIT count and species-level pan trap occupancy data. Both datasets were collected from 74 survey sites (N_{sites}) with 8 survey visits (N_{visit}) (four visits in each year 2017 and 2018). The average FIT counts and their standard deviation (in brackets) were calculated from the group-level FIT count data across all sites and visits and the average naive occupancy from the pantrap occupancy data across all species and sites. The number of species ($N_{species}$) in the species list for each insect group is also provided in the summary.

104 The above monitoring protocols generate two types of data, each collected at the same set of R indexed
 105 locations during replicated T number of visits at each site. One dataset comprises detection-nondetection
 106 data at the species level (henceforth 'species occupancy data'); the other is a count across all S species in the
 107 taxonomic group ('group count data').

108 2.2 State variables

109 We model species abundance as a spatial point process, in which the intensity of that point process determines
 110 the expected number of organisms per unit area. Let λ_{ij} be a latent variable describing the intensity of species
 111 j at location i and ψ_{ij} be the probability that species j occupies location i . We consider two ways by which
 112 the two latent variables can be linked in the IDM using the joint likelihood approach (Pacifiçi et al., 2017): the
 113 'shared' and the 'covariate' formulation.

114 2.2.1 Shared formulation

115 The intensity of each species is linked to the occupancy probability using the complementary log-log link
 116 function, which defines the probability that at least one organism is present (Kéry and Royle, 2015):

$$\begin{aligned} \log(\lambda_{ij}) &= \text{cloglog}(\psi_{ij}) = \beta_{0j} + \beta_{1j} \times \text{latitude}; \\ \beta_{0j} &\sim N(\mu_{\beta_0}, \sigma_{\beta_0}^2); \quad \beta_{1j} \sim N(\mu_{\beta_1}, \sigma_{\beta_1}^2), \end{aligned} \tag{1}$$

117 where β_{0j} the intercept for the species occupancy was normally distributed with mean μ_{β_0} and variance $\sigma_{\beta_0}^2$,
 118 β_{1j} the latitudinal gradient slope for species j was normally distributed with mean μ_{β_1} and variance $\sigma_{\beta_1}^2$. The
 119 hyperparameters of the intercept (μ_{β_0} and $\sigma_{\beta_0}^2$) and latitude effect (μ_{β_1} and $\sigma_{\beta_1}^2$) represent the community-level
 120 mean and variance parameters respectively in the IDM.

121 In this model structure, all the parameters are shared by the two latent states. Hence each dataset directly
 122 informs the latent state and both datasets provide equal weights to the joint likelihood of the IDM (Miller et al.,
 123 2019).

124 **2.2.2 Covariate formulation**

125 Although both FIT counts and pantrap surveys were performed by the same observer on the same survey visit,
 126 it makes sense for both latent variables to share covariates but allow each dataset to have separate intercepts
 127 because they have different survey protocols. The separate intercepts help model the average abundance and
 128 occupancy observation difference. Our use of the term "covariate formulation" differs slightly from previous
 129 studies (Pacifci et al., 2017; Miller et al., 2019), in which the term refers to using one dataset as a fixed effect
 130 in modelling the second dataset. In the classification of Miller et al. (2019), our covariate model is a form of
 131 joint-likelihood structure, but the term is useful to distinguish it from the shared formulation above.

132 The link function for the latent variables in this IDM framework becomes:

$$\begin{aligned}
 \text{cloglog}(\psi_{ij}) &= \beta_{0j} + \beta_{1j} \times \textit{latitude}; \\
 \log(\lambda_{ij}) &= \omega_0 + \beta_{1j} \times \textit{latitude}; \\
 \beta_{0j} &\sim N(\mu_{\beta_0}, \sigma_{\beta_0}^2); \\
 \beta_{1j} &\sim N(\mu_{\beta_1}, \sigma_{\beta_1}^2); \\
 \omega_0 &\sim N(\mu_{\omega_0}, \sigma_{\omega_0}^2),
 \end{aligned}
 \tag{2}$$

133 where β_{0j} the intercept for the species occupancy is normally distributed with mean μ_{β_0} and variance $\sigma_{\beta_0}^2$, ω_0
 134 the intercept of the group counts is normally distributed with mean μ_{ω_0} and variance $\sigma_{\omega_0}^2$, β_{1j} the slope of the
 135 latitudinal gradient for species j is normally distributed with mean μ_{β_1} and variance $\sigma_{\beta_1}^2$. As described for
 136 the shared model (section 2.2.1), the intercept and covariate effect hyperparameters represent their respective
 137 community-level mean and variance parameters in the models.

138 The covariate structure allows both state variable models in the IDM to share important parameters but
 139 preserve their average abundance when no covariate effects exist. Moreover, the quality of both datasets
 140 determines how well the parameters are estimated (Pacifci et al., 2017) since some parameters will be estimated
 141 using each dataset, and the parameters that are not shared serve as (unequal) weights for the contribution from
 142 each dataset.

143 **2.3 Sub-models for each dataset**

144 Having defined the latent state variables λ_{ij} and ψ_{ij} and the possible ways they can be linked together, the
145 sub-models for species occupancy data (section 2.3.1) and group-level count data (section 2.3.2) can be defined.
146 In addition, the model can estimate various community ecology metrics (see section 2.5) as derived parameters.
147 Based on preliminary analysis (Supplementary information 1), we used a negative binomial model with an
148 intercept and covariate to fit the group count data. We also used logistic regression with intercept, covariate
149 effect, site and visit random effect to fit the species occupancy data.

150 **2.3.1 Sub-models for species occupancy data**

151 We model the species occupancy data with an occupancy-detection model (MacKenzie et al., 2002). The true
152 ecological state (true presence or absence denoted as z in this study) for species j at site i is modelled with
153 a Bernoulli distribution with probability ψ_{ij} , where ψ_{ij} was the probability of species j occupying site i as
154 defined by equations (1) and (2).

155 The detection probability (p_{ijk}) for species j at site i during the survey visit k is modelled with a site,
156 species and visit random effect logistic regression using the logit link. That is:

$$\begin{aligned} \text{logit}(p_{ijk}) &= \zeta_i + \nu_j + \rho_k; \\ \zeta_i &\sim N(0, \sigma_\zeta^2) \quad \text{and} \quad \nu_j \sim N(0, \sigma_\nu^2) \quad \rho_k \sim N(0, \sigma_\rho^2), \end{aligned} \tag{3}$$

157 where ζ_i , the effect of site i , is normally distributed with zero mean and variance σ_ζ^2 ; ν_j , the effect of species
158 j , is normally distributed with zero mean and variance σ_ν^2 ; and ρ_k , the effect of survey visit k , is normally
159 distributed with mean 0 and variance σ_ρ^2 . We model the visit effect in the detection process to account for
160 the significant visit effect found during the exploration phase for the species occupancy data (Supplementary
161 information 1). By the definition of our model for the detection probability in equation (3), the average
162 detection probability for a species in any given site is 0.5, which allows all species in the taxonomic group to
163 have an equal chance of being detected or not detected on average.

164 Let the observation for species j during the k^{th} visit to location i be represented by X_{ijk} , for $i =$
165 $1, 2, \dots, R$ indexed sites and $j = 1, 2, \dots, S$ species. This observation, over the five pantrap replicates at each

166 site, is Binomially distributed with probability $z_{ij} \times p_{ijk}$, where p_{ijk} is the detection probability and z_{ij} is the
167 true state of species j at site i (that is, $X_{ijk} \sim \text{Binomial}(5, z_{ij} \times p_{ijk})$).

168 **2.3.2 Sub-model for group count data**

169 Having defined the intensity of species j at location i (equations (1) and (2)), the intensity for the group counts
170 will be a sum of all the intensities of the species that make up that taxonomic level. This is because we assume
171 the group counts are made up of all the species in the pantrap data, and the sum of realisations from Poisson
172 point processes is also a Poisson point process with an intensity equal to the sum of the intensities of the
173 individual components (Harremoës, 2001; Jacod, 1975).

174 Let Y_{ik} be the observed count of individuals on the k th survey (across all species in the group). We
175 modelled the counts with a negative binomial distribution (to allow for extra variation in the count data)
176 with parameters θ and $\gamma = \frac{\theta}{\theta + \lambda_i^g}$, where $\lambda_i^g = \sum_j^S \lambda_{ij}$ is the intensity of the group counts at site i (that
177 is, $Y_{ik} \sim \text{NB}(\theta, \gamma)$). The parameter θ is the overdispersion parameter, which allows us to model the extra
178 variation in the group count data. Note that as $\theta \rightarrow \infty$, the negative binomial distribution converges upon the
179 Poisson distribution.

180 We present the various joint likelihood structures defined in section (2.2) and the sub-models for each
181 PoMS dataset defined in section (2.3) in Figure 1.

182 **2.4 Community Diversity Indices**

183 The community alpha diversity was estimated using the Shannon-Wiener diversity index. This is the most
184 commonly used index from the Hills indices (Hill, 1973), and it places equal weights on rare and dominant
185 species. We acknowledge that the Shannon-Wiener diversity index may have some limitations (Lande, 1996;
186 Morishita, 1996; Itô, 2007; Gatti et al., 2020; Chao and Jost, 2015; O'hara, 2005), in which case other indices
187 such as Simpson index may be preferable. However, we use the Shannon-Wiener diversity index to show
188 how alpha diversity can be estimated using our proposed IDM and how all the models capture the true alpha
189 diversity. For real-world applications, we urge caution about the choice of the index. Moreover, the Hills
190 indices are all functions of the relative abundance proportion, so the method developed for one index can be

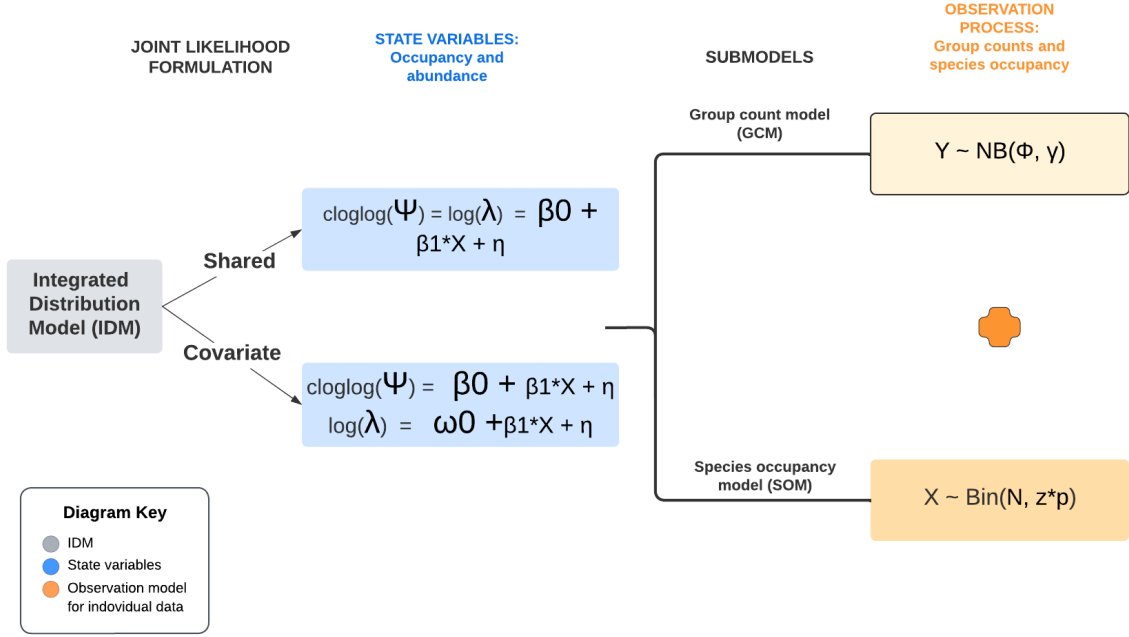


Figure 1: Flowchart showing the integrated distribution model process for the PoMS survey data. To fit the IDM, we used two joint likelihood links in this study: shared formulation (section 2.2.1) and covariate formulation (section 2.2.2). The state variables models are defined by equations (1) and (2). The sub-models for each dataset: the group count model (GCM) and species occupancy model (SOM) have been defined as the observation process of abundance and occupancy respectively (sections 2.3.2 and 2.3.1 respectively). The IDM combines the SOM and GCM for each joint likelihood link used. All the parameters in this flowchart are defined in sections 2.2 and 2.3. In addition to the intercept and covariate effect, we add a species interaction effect η in this flowchart.

191 easily extended to the others. The Shannon-Wiener diversity index was calculated as:

$$H^1 = - \sum_{j=1}^S r_{ij} \log(r_{ij}), \quad (4)$$

192 where $r_{ij} = \frac{\lambda_{ij}}{\sum_{j=1}^S \lambda_{ij}}$ is the relative abundance of a species j at location i .

193 2.5 Evaluating model performance

194 We fitted five models to the PoMS survey data in this study: IDM and group count model (GCM) with the
 195 shared formulation of the joint likelihood defined in section 2.2.1 which we will refer to as **IDMSH** and
 196 **GCMSh** respectively, the IDM and GCM with covariate formulation of the joint likelihood defined in section

197 2.2.2 which we will refer to as **IDMCO** and **GCMCO** respectively, and the species occupancy model (**SOM**).
198 The two IDMs (IDMSH and IDMCO) fitted a joint likelihood model with both the occupancy and group count
199 data; the two GCMs (GCMSH and GCMCO) fitted the negative binomial regression model to the group count
200 data with the two joint likelihood formulations, and SOM fitted the sub-model for the species occupancy
201 data (section 2.4.1). We note that the alpha diversity estimates from the GCMs are strongly driven by the
202 priors assigned to the parameters of λ_{ij} . In the absence of information in the data to contradict this prior, we
203 anticipate that GCMs will estimate the local alpha diversity very poorly. We recognise that this model is not
204 something that community ecologists would choose to fit, but the comparison with other models is informative.
205 These models are summarised in Table 2.

| Model | Model description | Type | Data used | Predictor |
|-------|---|------------|-----------|--|
| IDMSH | IDM with shared structure defined in equation (1) | Integrated | GC and SO | $\beta_{0j} + \beta_{1j} \times lat_i$ |
| IDMCO | IDM with shared structure defined in equation (2) | | | $\beta_{0j} + \beta_{1j} \times lat_i$ $\omega_0 + \beta_{1j} \times lat_i$ |
| GCMSH | GCM with shared structure defined in equation (1) | Single | GC | $\beta_{0j} + \beta_{1j} \times lat_i$ |
| GCMCO | GCM with shared structure defined in equation (2) | | | $\omega_0 + \beta_{1j} \times lat_i$ |
| SOM | species occupancy model | Single | SO | $\beta_{0j} + \beta_{1j} \times lat_i$ |

Table 2: Models fitted in this study, their descriptions, predictors, type and data used to fit them. Two integrated models: IDMSH and IDMCO, and three single models: GCMSH, GCMCO and SOM, are fitted. The data used are from the UK PoMS survey: FIT counts (GC) and Pantrap species occupancy (SO) data. The cloglog link was used for the occupancy model and the log link was used for the group count model. The definitions of the parameters used in the predictor column are described in section (2.3), with *lat* referring to the latitudinal gradient slope.

206 2.5.1 Fitting the models

207 We fitted the models in a Bayesian framework. We obtained samples of the parameters using the Markov
208 chain Monte Carlo (MCMC) approach and estimated posterior summaries of model parameters using the
209 NIMBLE package (de Valpine et al., 2017) in *R* (R Core Team, 2022). We chose a normal distribution with
210 zero mean and variance of 100 as the prior for the mean hyperparameters of the state variables and an inverse
211 gamma distribution with scale parameter 2 and shape parameter 1 as the prior distribution for the variance

212 hyperparameters. We ran three chains with 300000 iterations for all the models, and 200000 were discarded
 213 as burn-in samples. We keep a twentieth of the left-over samples to reduce the hard disk space used by our
 214 analysis. The convergence of the fitted model was checked by estimating Gelman-Rubin R-hat statistic (Brooks
 215 and Gelman, 1998) using the ggmcmc package (Fernández-i Marín, 2013) and rejected the models with R-hat
 216 greater than 1.1.

217 2.5.2 Simulation study

218 We performed simulation studies to assess which of the five models (described in Table 2) better estimated
 219 the true alpha diversity. We simulated 30 data replicates using the IDM framework for each latent variable
 220 formulation used in this study (i.e. using both the covariate and the shared formulation). We used the same
 221 number of sites and visits from the PoMS surveys but used 20 species for the simulations due to computational
 222 expensiveness in running the models for more species.

223 The true values for the hyperparameters defined in sections 2.2 were chosen as follows: $\mu_{\beta_0} = 0$,
 224 $\sigma_{\beta_0} = 0.2$, $\mu_{\beta_1} = -2$, $\sigma_{\beta_1} = 1$, $\sigma_{\omega_0} = 0.2$, $\sigma_{\zeta} = 0.3$, $\sigma_{\nu} = 1$ and $\sigma_{\rho} = 2$. We also randomly selected 25
 225 sites for each visit in the group count and occupancy model and assigned them *NAs* to reflect missing species
 226 identifications and group counts in the PoMS data.

227 We fitted the five study models defined in Table 2 to the 30 simulated datasets for each joint likelihood
 228 formulation. By this, we employed a cross-design to ascertain the effect of fitting a wrong model in this study.
 229 For example, when the IDMC0 or GCMCO is fitted to the dataset simulated under the shared formulation,
 230 we can infer the effect of fitting a covariate-formulated model ("wrong model") to the dataset. We assessed
 231 this effect by estimating the mean bias and precision of Shannon estimates at each site across the replicated
 232 datasets. That is, for each site i , we obtain the metrics:

$$\begin{aligned} \text{Mean bias} &= \frac{1}{30} \sum_{k=1}^{30} (\hat{H}'_i^{(k)} - H_i^{(k)}), \\ \text{Mean precision} &= \frac{1}{30} \sum_{k=1}^{30} \frac{1}{SD(\hat{H}'_i^{(k)})^2}, \end{aligned} \tag{5}$$

233 where $\hat{H}'_i^{(k)}$ is the posterior mean of the Shannon index for dataset k , $H_i^{(k)}$ is the true Shannon index obtained
 234 from simulating dataset k and $SD(\hat{H}'_i^{(k)})$ is the posterior standard deviation of the Shannon index for dataset

235 k . The fitted models with mean bias closer to 0 and the highest mean precision are indicated to perform best.

236 **2.5.3 Model Validation and Assessment**

237 **Model predictive performance**

238 We performed two-fold cross-validation to ascertain the model's ability to predict new data. The same
239 folds are used for all the models under study, and the log pointwise predictive density (Nicenboim et al.,
240 2021; Gelman et al., 2014) was used to measure the cross-validation's predictive accuracy. The log pointwise
241 predictive density (lppd) is defined as:

$$lppd = \frac{1}{K} \sum_{k=1}^K \sum_{n=1}^N \log(P(y_{n,k}|y_{-n,k}, \hat{\theta}, M)) \quad (6)$$

242 where $\log(P(y_{n,k}|y_{-n,k}, \hat{\theta}, M))$ is the log predictive density of the withheld data samples $y_{n,k}$ in fold k under
243 model M , which was trained with data samples $y_{-n,k}$ in fold k to obtain estimated model parameters $\hat{\theta}$ with n
244 being the number of samples in each fold and N is the number of samples of each fold. Larger values of the
245 metric indicate better performance.

246 It must be pointed out that the withheld samples used in IDMSH and IDMCO have both species occupancy
247 (X) and group count (Y) samples in their training and validation sets. Therefore, we estimated the lppd for
248 the validation samples from the pantrap and group count data separately after we had estimated the model
249 parameters $\hat{\theta}$ with both datasets in the training samples. Since the log predictive density is additive (Gelman
250 et al., 2014), the log predictive density of the integrated model was obtained by summing the lppd of each
251 dataset.

252 **Information provided by each dataset**

253 We also ascertained the information contributed to the IDM by each data type. This was done by comparing
254 the log-likelihoods of the single models (SOM and GCMs) to that of the IDMs (where both single and integrated
255 models being compared share the same joint likelihood structure), following Zulian et al. (2021). Since there
256 are two data types in this study: pantrap data and FIT count data, including a data type that informs the
257 IDMs should lead to better predictions (higher prediction accuracy) of the other data types. For example, by
258 comparing the predictive log-likelihoods of the GCMCO to IDMCO for group count data, one can assess
259 whether the pantrap occupancy data improves the predictive performance of IDMCO on the group count data.

260 We shall refer to this approach as the 'marginal contribution' of a data type in the rest of this paper. Negative
261 values of the marginal contribution indicate that the data type did not contribute to the IDM.

262 It must be stated that the marginal contribution can only indicate whether a data type provides information.
263 Due to differences in the data types (occupancy and count data) and sample sizes, it is unfeasible to compare
264 the marginal contribution of the data types to ascertain which one provides the most information.

265 **3 Results**

266 The estimates of the mean bias and precision of Shannon diversity estimates over all 30 replicated simulated
267 datasets are presented in Figure 2. The log-predictive density from the two-fold cross-validation and average
268 Shannon index across all the study sites are summarised in Table 3. The site-specific precision estimates of the
269 Shannon indices for each insect group and the model used to fit the data are presented in Figure 3. All other
270 figures and tables referred to in this section are presented in Supplementary Information 2.

271 **3.1 Simulation study**

272 Figure 2 shows the distribution of the mean bias and precision of the Shannon indices at the 74 sites estimated
273 from the five study models fitted to the simulated data described in section 2.5.2. Whether the data were
274 simulated under the shared or covariate formulations, the mean bias of the Shannon index from the integrated
275 models (irrespective of their joint likelihood structure) was similar to that from SOM, with the median bias
276 around 0 with small variation across sites. This suggested that the integrated models and SOM well captured
277 the true Shannon index across all the study sites.

278 As expected, the Shannon indices were poorly estimated the GCMs. Alpha diversity was consistently
279 overestimated by the GCMCO model and underestimated by GCMSH (Figure 2), and both models have much
280 lower precision than other models. As explained in the Methods, this is expected because the only information
281 about species identities in these models derives from the priors.

282 Although the mean bias of the Shannon indices from the integrated models and SOM are similar, the
283 Shannon indices were estimated with higher precision in the integrated models than in SOM (blue bars in
284 Figure 2). When the data was simulated under the covariate formulation (red bars), the precision of Shannon
285 diversity estimates from the integrated models was similar to that of SOM.

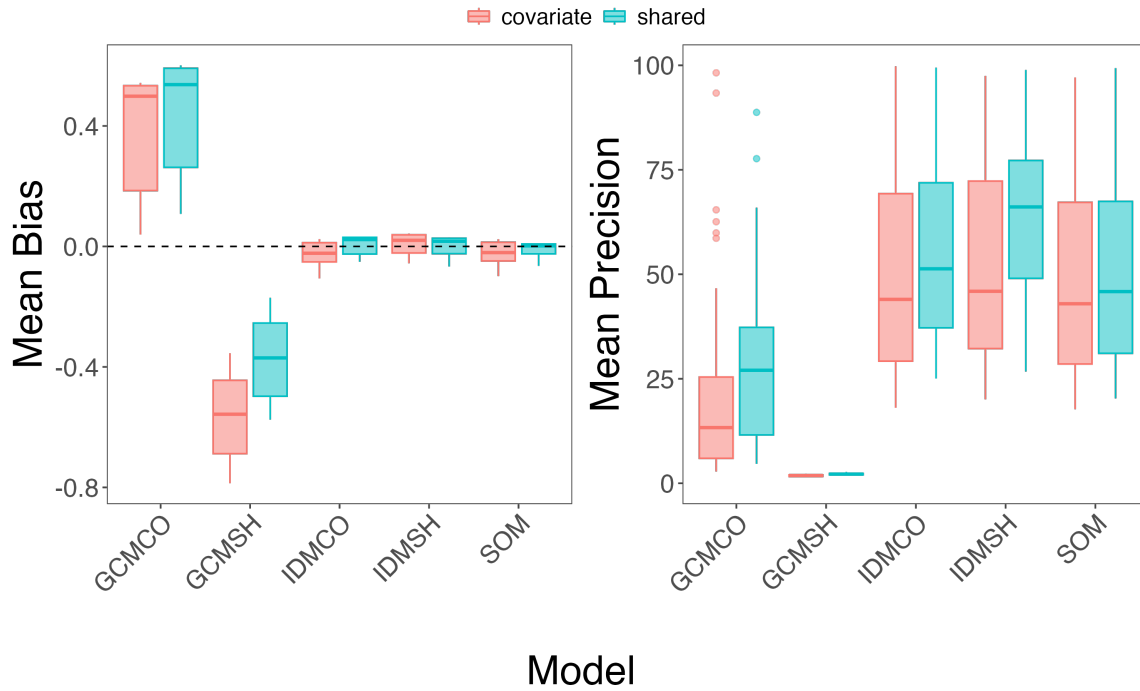


Figure 2: Mean bias and precision of Shannon index from the five study models fitted to the simulated data. The boxplot shows the distribution of the mean bias and precision for the 74 sites. The five models: two integrated models (IDMSH and IDMCO), two group count models (GCMCO and GCMSH) and a species occupancy model (SOM) were fitted to data simulated under the shared structure (coloured in blue) and those simulated under the covariate structure (red).

286 3.2 Analysis of PoMS dataset

287 3.2.1 Estimation of Shannon index (H')

288 Shannon diversity is expected to be higher for communities with a comparatively higher number of species
 289 (Roswell et al., 2021) and/or evenness (Nagendra, 2002). It is, therefore, not surprising that the Shannon
 290 indices were highest for hoverflies ($n = 79$ species) and lowest for bumblebees ($n = 17$ species; Tables 1 and 3).

291 The estimates of H' from the five models showed consistencies in the estimated diversity pattern for each
 292 insect group, as we observe in Table 3 and Supplementary information 2 Figure S2-1. Firstly, there was a
 293 negative latitudinal effect on the estimates of the Shannon indices (that is, the Shannon index decreased with
 294 the latitudinal gradient; Figure S2-2). The community intercept (μ_{ω_0}) estimated from GCMCO and IDMCO
 295 were relatively the same, but the estimated latitudinal and species effect (μ_{β_1} and μ_{β_0} respectively) from the
 296 integrated models lies between those estimated from the group count and species occupancy models (Figure

| Insect group | Model | Shannon index | | log predictive density | | | Marginal Contribution | |
|---------------|--------|---------------|-------|------------------------|------------------|----------------|-----------------------|-------------|
| | | Mean | SD | All dataset | Pantrap | FIT count | Pantrap | FIT count |
| Bumblebees | GCM SH | 2.79 | 0.02 | - | - | -239.90 | - | - |
| | GCM CO | 2.78 | 0.06 | - | - | -290.15 | - | - |
| | SOM | 1.08 | 0.17 | - | -3649.25 | - | - | - |
| | IDM SH | 2.29 | 0.07 | -3561.26 | -3322.39 | -238.90 | 326.86 | 1.0 |
| | IDM CO | 1.86 | 0.08 | -3489.85 | -3250.97 | -238.87 | 398.28 | 1.03 |
| Hoverflies | GCM SH | 4.34 | 0.014 | - | - | -517.49 | - | - |
| | GCM CO | 4.32 | 0.05 | - | - | -513.62 | - | - |
| | SOM | 3.98 | 0.13 | - | -35118.55 | - | - | - |
| | IDM SH | 4.01 | 0.08 | -36195.10 | -35715.74 | -479.36 | 38.14 | -597 |
| | IDM CO | 4.03 | 0.09 | -32275.90 | -31716.42 | -559.48 | -45.86 | 3402 |
| Solitary bees | GCM SH | 4.10 | 0.08 | - | - | -150.51 | - | - |
| | GCM CO | 4.08 | 0.18 | - | - | -446.05 | - | - |
| | SOM | 3.04 | 0.40 | - | -14372.42 | - | - | - |
| | IDM SH | 3.25 | 0.33 | -11341 | -11165.97 | -175.39 | 3206.45 | -24.88 |
| | IDM CO | 3.27 | 0.31 | -11464.48 | -11285.78 | -178.70 | 3086.64 | -28.19 |

Table 3: Log predictive density from the two-fold cross-validation, the marginal contribution of each dataset and the Bayesian p-values from the posterior predictive checks of all the models fitted to the PoMS dataset. For each insect group, the marginal contribution of pantrap data was estimated as $lppd_{SOM} - lppd_{IDM_{SH}}$ and $lppd_{SOM} - lppd_{IDM_{CO}}$; and the marginal contribution of FIT count data was estimated as the $lppd_{GCM_{SH}} - lppd_{IDM_{SH}}$ and $lppd_{GCM_{CO}} - lppd_{IDM_{CO}}$.

297 S2-2). Additionally, the group count models (GCM SH and GCM CO) had the highest average H' estimates
298 (Table 3), followed by the integrated models (IDM SH and IDM CO) and finally, the species occupancy model
299 (SOM). These observations suggested that the integrated models serve as the average model for the species
300 occupancy and group count models.

301 We have already established from the simulation study that the priors strongly affect the Shannon indices
302 estimated from the GCM models. Narrowing our observations to the site-specific precision estimates of the
303 Shannon indices from the integrated models and SOM, we observed the estimates from the integrated models
304 were more precise than those from SOM (Figure 3). This precision was also higher for the sites with higher
305 Shannon diversity estimates (compare Figure 3 to Supplementary information 2 Figure S2-1).

306 3.2.2 Predictive Performance and information provided

307 Table 3 shows the two-fold cross-validation log-predictive density estimated from the five study models for
308 the three insect groups: bumblebees, solitary bees and hoverflies. For bumblebees, we find that both IDMs
309 outperform the single-dataset models in predicting both the pantrap and FIT count data. For hoverflies, the

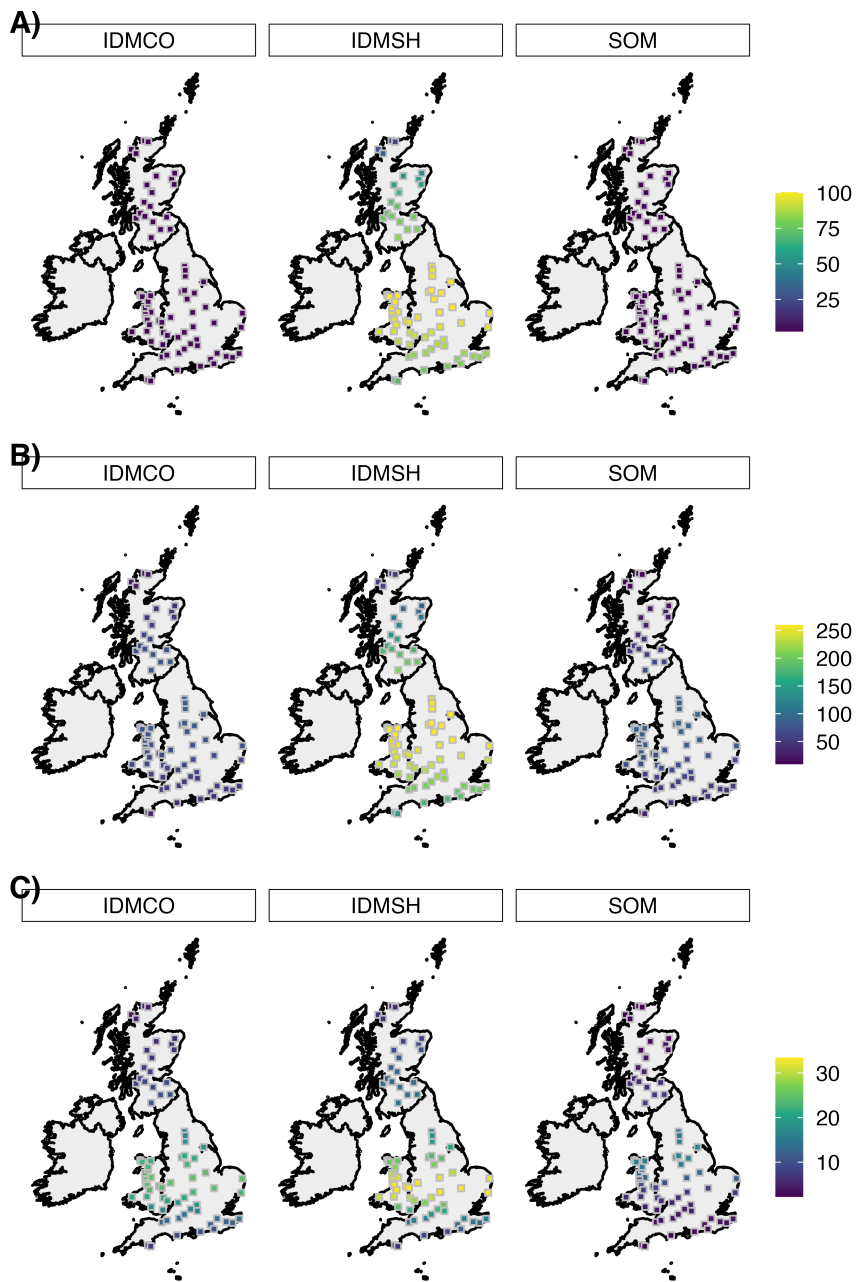


Figure 3: Precision of the Shannon diversity (H') estimates for each of the 74 PoMS sites from the five models in this study summarised in Table (2) for each of the insect groups: A) bumblebees, B) hoverflies and C) solitary bees.

310 best fitting model in each case is an IDM, with the covariate formulated model (IDMCO) performing best for
311 pantrap data and the shared formulated model performing best for the FIT counts. For solitary bees, we find
312 that both IDMs outperform the SOM for predicting the pantrap data, but that one of the group count models is
313 the best predictor of the FIT count data. These results show that the IDMs outperformed the single models in
314 the prediction accuracy of new data for bumblebees and hoverflies and at least as well for the solitary bees. In
315 other words, the inclusion of FIT Count data from has added information to the models.

316 Table 3 also shows the marginal contribution of each dataset to the integrated models. For the models fitted
317 to the bumblebees and hoverflies, both pantrap and FIT count data contributed to the IDM (with a positive
318 marginal contribution), but the contribution was higher in IDMCO than IDMSH. For solitary bees, the marginal
319 contribution of the FIT count was negative for both IDMCO and IDMSH (indicating they do not provide
320 information into the IDM) and the marginal contribution of the pantrap data was positive, indicating that the
321 FIT count data did not inform the IDMs. This was expected since the average FIT counts of bumblebees and
322 hoverflies (1.11 ± 5.18 and 2.74 ± 10.92 respectively), were significantly higher than that of the solitary bees
323 (0.29 ± 1.62 ; Table 1). There was much information from this count data to inform the IDMs to predict the
324 pantrap data better for bumblebees and hoverflies.

325 **4 Discussion**

326 Many data types are available in community ecology, and many modelling techniques are available to analyse
327 data types separately. In some cases, multiple datasets are available that differ in taxonomic resolution. We
328 developed an integrated distribution model that combined data from different taxonomic levels to estimate
329 alpha diversity in a community. Using a combination of simulations and analysis of empirical data, we showed
330 that integrated models can produce useful estimates of community ecology parameters from datasets that lack
331 the information to do so if analysed separately. In addition, the IDMs performed better than the single models
332 in most cases.

333 Previous studies have shown that IDMs perform better than single models in estimating state variable
334 parameters and prediction accuracy of new datasets (Strebel et al., 2022; Pacifici et al., 2017; Doser et al., 2022;
335 Miller et al., 2019). Although Miller et al. (2019) noted that IDMs present opportunities to model community
336 dynamics and diversity from multiple datasets, our study is the first to implement this by combining data

337 from different taxonomic levels (species and group level). Our simulation and case studies showed that the
338 IDMs outperform the single models in producing precise alpha diversity estimates in a community if both
339 datasets share information between them (Figure 2, Supplementary information 2 Figure S2-1 and Table 3).
340 The information from each dataset was shared through the joint likelihood framework, and the information
341 sharing process has been noted in the literature to be the benefit of using IDMs (Isaac et al., 2020; Miller et al.,
342 2019).

343 Furthermore, the proposed IDMs outperform the single models' prediction accuracy of new datasets for
344 some insect groups. From our model assessment of the PoMS data using two-fold cross-validation, IDMs
345 outperformed the single models in predicting new data for all insect groups, except the solitary bees FIT count
346 data (Table 3). The out-performance is evident from the information provided by each dataset into the IDM to
347 inform the estimation of the model parameters directly. This observation is well noted in literature (Zulian
348 et al., 2021). For instance, when modelling the solitary bees dataset, pantrap data did not inform the IDM to
349 predict the FIT count data better, and as such the group count model outperforms the IDMs (Table 3).

350 In this study, we explored two IDM variants with different joint likelihood formulations. The covariate
351 and shared formulations had very similar performance in terms of predictive performance and alpha diversity
352 estimation but differed in how well they fit the two datasets. The shared joint likelihood structure ensured
353 that all state variables were shared between both datasets. The covariate structure allowed some flexibility in
354 sharing the state model definition by allowing each dataset to have a unique intercept. Previous studies on
355 IDMs, using either covariate and shared joint likelihood structures, have all shown that IDMs have higher
356 prediction accuracy than single models (Koshkina et al., 2017; Zulian et al., 2021; Fletcher Jr et al., 2019;
357 Fletcher et al., 2016; Pacifici et al., 2017; Simmonds et al., 2020; Adde et al., 2021; Ahmad Suhaimi et al.,
358 2021). These methods have been used to model species distributions and turnover using multiple data types
359 from the same taxonomic levels. Just a few of these studies (such as Chevalier et al., 2021) exist that explore
360 various joint likelihood structures for their IDMs. Our study showed that the choice of structure has little effect
361 on the IDM's predictive performance over the single models since all the IDMs outperform the single models,
362 except for solitary bees FIT count data (Table 3). Additionally, the pattern of estimated Shannon diversity and
363 the precision of the estimates was invariant to the choice of the joint likelihood structure (Figures 2 and 3 and
364 Table 3). This indicates the choice of the joint likelihood formulation is inconsequential to the performance of
365 IDMs, and any alternative can be chosen to model alpha diversity.

366 The UK PoMS protocols are specifically designed to produce datasets with different taxonomic resolutions.
367 New monitoring technologies create many situations in which analysts might encounter datasets that differ
368 in taxonomic resolution. For example, data on the abundance of aquatic macroinvertebrates, such as those
369 collected by kick-sampling for Water Framework Directive reporting, are typically reported at the genus level
370 or higher (Haase et al., 2023). Modern DNA (meta)barcoding makes it possible to identify specimens in these
371 samples to species level, but typically only as presence-absence data (Bohan et al., 2017). Another promising
372 use case is the combination of traditional field surveys with data identified from images using computer vision:
373 algorithms often have low confidence in the species identity, but high confidence in the Genus. Our model
374 provides a ready-made solution for estimating community parameters in such situations.

375 Other situations might arise in which mixed taxonomic resolution is an unwanted byproduct of the data
376 generation process. A good example would be a citizen science projects where participants differ in their
377 taxonomic skill levels, such that some report counts at species level but others report at a coarser level. Our
378 approach provides a way to use all the data at the resolution at which it was captured. Thus, our proposed
379 model further extends the range of applications for IDMs in ecology and conservation to help researchers and
380 conservationists make the most of available data, in order to provide better evidence and understanding about
381 biodiversity.

382 **Data availability**

383 The code and PoMS dataset used is available on GitHub repository: [https://github.com/Peprah94/Integrated-](https://github.com/Peprah94/Integrated-distribution-models-for-different-taxonomic-levels)
384 [distribution-models-for-different-taxonomic-levels](https://github.com/Peprah94/Integrated-distribution-models-for-different-taxonomic-levels) with DOI:10.5281/zenodo.8424494.

385 **Conflict of Interest**

386 The authors declare no conflict of interest.

387 **Author Contribution**

388 All the authors were involved in the idea conception and manuscript writing. KPA, RBO and NI were involved
389 with the methodology development, KPA run the entire analysis and led the writing of the manuscript.

References

- 391 Abadi, F., Gimenez, O., Arlettaz, R. and Schaub, M. (2010) An assessment of integrated population models:
392 bias, accuracy, and violation of the assumption of independence. *Ecology*, **91**, 7–14.
- 393 Adde, A., Casabona i Amat, C., Mazerolle, M. J., Darveau, M., Cumming, S. G. and O’Hara, R. B. (2021)
394 Integrated modeling of waterfowl distribution in western Canada using aerial survey and citizen science
395 (eBird) data. *Ecosphere*, **12**, e03790.
- 396 Ahmad Suhaimi, S. S., Blair, G. S. and Jarvis, S. G. (2021) Integrated species distribution models: A
397 comparison of approaches under different data quality scenarios. *Diversity and Distributions*, **27**, 1066–
398 1075.
- 399 Alexander, N., Moyeed, R. and Stander, J. (2000) Spatial modelling of individual-level parasite counts using
400 the negative binomial distribution. *Biostatistics*, **1**, 453–463.
- 401 Baselga, A. (2010) Partitioning the turnover and nestedness components of beta diversity. *Global ecology and*
402 *biogeography*, **19**, 134–143.
- 403 Besbeas, P., Freeman, S. N., Morgan, B. J. and Catchpole, E. A. (2002) Integrating mark–recapture–recovery
404 and census data to estimate animal abundance and demographic parameters. *Biometrics*, **58**, 540–547.
- 405 Bhattacharya, A. and Dunson, D. B. (2011) Sparse Bayesian infinite factor models. *Biometrika*, 291–306.
- 406 Bird, T. J., Bates, A. E., Lefcheck, J. S., Hill, N. A., Thomson, R. J., Edgar, G. J., Stuart-Smith, R. D.,
407 Wotherspoon, S., Krkosek, M., Stuart-Smith, J. F. et al. (2014) Statistical solutions for error and bias in
408 global citizen science datasets. *Biological Conservation*, **173**, 144–154.
- 409 Bohan, D. A., Vacher, C., Tamaddon-Nezhad, A., Raybould, A., Dumbrell, A. J. and Woodward, G. (2017)
410 Next-generation global biomonitoring: large-scale, automated reconstruction of ecological networks. *Trends*
411 *in ecology & evolution*, **32**, 477–487.
- 412 Breeze, T. D., Bailey, A. P., Balcombe, K. G., Brereton, T., Comont, R., Edwards, M., Garratt, M. P., Harvey,
413 M., Hawes, C., Isaac, N. et al. (2021) Pollinator monitoring more than pays for itself. *Journal of Applied*
414 *Ecology*, **58**, 44–57.

- 415 Broms, K. M., Hooten, M. B. and Fitzpatrick, R. M. (2015) Accounting for imperfect detection in hill numbers
416 for biodiversity studies. *Methods in Ecology and Evolution*, **6**, 99–108.
- 417 Brooks, S. P. and Gelman, A. (1998) General methods for monitoring convergence of iterative simulations.
418 *Journal of computational and graphical statistics*, **7**, 434–455.
- 419 Chambert, T., Rotella, J. J. and Higgs, M. D. (2014) Use of posterior predictive checks as an inferential
420 tool for investigating individual heterogeneity in animal population vital rates. *Ecology and Evolution*, **4**,
421 1389–1397.
- 422 Chao, A. and Jost, L. (2015) Estimating diversity and entropy profiles via discovery rates of new species.
423 *Methods in Ecology and Evolution*, **6**, 873–882.
- 424 Chevalier, M., Broennimann, O., Cornuault, J. and Guisan, A. (2021) Data integration methods to account for
425 spatial niche truncation effects in regional projections of species distribution. *Ecological Applications*, **31**,
426 e02427.
- 427 Del Toro, I., Ribbons, R. R., Hayward, J. and Andersen, A. N. (2019) Are stacked species distribution models
428 accurate at predicting multiple levels of diversity along a rainfall gradient? *Austral Ecology*, **44**, 105–113.
- 429 Doser, J. W., Leuenberger, W., Sillett, T. S., Hallworth, M. T. and Zipkin, E. F. (2022) Integrated community
430 occupancy models: A framework to assess occurrence and biodiversity dynamics using multiple data
431 sources. *Methods in Ecology and Evolution*, **13**, 919–932.
- 432 Durante, D. (2017) A note on the multiplicative gamma process. *Statistics & Probability Letters*, **122**, 198–204.
- 433 Fletcher, R. J., McCleery, R. A., Greene, D. U. and Tye, C. A. (2016) Integrated models that unite local and
434 regional data reveal larger-scale environmental relationships and improve predictions of species distributions.
435 *Landscape Ecology*, **31**, 1369–1382.
- 436 Fletcher Jr, R. J., Hefley, T. J., Robertson, E. P., Zuckerberg, B., McCleery, R. A. and Dorazio, R. M. (2019) A
437 practical guide for combining data to model species distributions. *Ecology*, **100**, e02710.
- 438 Gatti, R. C., Amoroso, N. and Monaco, A. (2020) Estimating and comparing biodiversity with a single
439 universal metric. *Ecological Modelling*, **424**, 109020.

- 440 Gelman, A., Hwang, J. and Vehtari, A. (2014) Understanding predictive information criteria for bayesian
441 models. *Statistics and computing*, **24**, 997–1016.
- 442 Gotelli, N. J. and Chao, A. (2013) Measuring and estimating species richness, species diversity, and biotic
443 similarity from sampling data.
- 444 Guillera-Arroita, G., Kéry, M. and Lahoz-Monfort, J. J. (2019) Inferring species richness using multispecies
445 occupancy modeling: Estimation performance and interpretation. *Ecology and Evolution*, **9**, 780–792.
- 446 Haase, P., Bowler, D. E., Baker, N. J., Bonada, N., Domisch, S., Garcia Marquez, J. R., Heino, J., Hering, D.,
447 Jähnig, S. C., Schmidt-Kloiber, A. et al. (2023) The recovery of european freshwater biodiversity has come
448 to a halt. *Nature*, 1–7.
- 449 Harremoës, P. (2001) Binomial and poisson distributions as maximum entropy distributions. *IEEE Transactions*
450 *on Information Theory*, **47**, 2039–2041.
- 451 Hill, M. O. (1973) Diversity and evenness: a unifying notation and its consequences. *Ecology*, **54**, 427–432.
- 452 Hooten, M. B. and Hobbs, N. T. (2015) A guide to bayesian model selection for ecologists. *Ecological*
453 *monographs*, **85**, 3–28.
- 454 Isaac, N. J., Jarzyna, M. A., Keil, P., Dambly, L. I., Boersch-Supan, P. H., Browning, E., Freeman, S. N.,
455 Golding, N., Guillera-Arroita, G., Henrys, P. A. et al. (2020) Data integration for large-scale models of
456 species distributions. *Trends in ecology & evolution*, **35**, 56–67.
- 457 Itô, Y. (2007) Recommendations for the use of species diversity indices with reference to a recently published
458 article as an example. *Ecological research*, **22**, 703–705.
- 459 Jacod, J. (1975) Two dependent poisson processes whose sum is still a poisson process. *Journal of Applied*
460 *Probability*, **12**, 170–172.
- 461 Jost, L. (2007) Partitioning diversity into independent alpha and beta components. *Ecology*, **88**, 2427–2439.
- 462 Jost, L., DeVries, P., Walla, T., Greeney, H., Chao, A. and Ricotta, C. (2010) Partitioning diversity for
463 conservation analyses. *Diversity and Distributions*, **16**, 65–76.

- 464 Kéry, M. and Royle, J. A. (2015) Applied hierarchical modeling in ecology: Analysis of distribution, abundance
465 and species richness in r and bugs.
- 466 — (2020) *Applied hierarchical modeling in ecology: Analysis of distribution, abundance and species richness*
467 *in R and BUGS: Volume 2: Dynamic and advanced models*. Academic Press.
- 468 Koshkina, V., Wang, Y., Gordon, A., Dorazio, R. M., White, M. and Stone, L. (2017) Integrated species
469 distribution models: combining presence-background data and site-occupancy data with imperfect detection.
470 *Methods in Ecology and Evolution*, **8**, 420–430.
- 471 Lahti, L., Shetty, S. and Ernst, F. (2021) Orchestrating microbiome analysis.
- 472 Lande, R. (1996) Statistics and partitioning of species diversity, and similarity among multiple communities.
473 *Oikos*, 5–13.
- 474 Loeys, T., Moerkerke, B., De Smet, O. and Buysse, A. (2012) The analysis of zero-inflated count data: Beyond
475 zero-inflated poisson regression. *British Journal of Mathematical and Statistical Psychology*, **65**, 163–180.
- 476 MacKenzie, D. I. and Bailey, L. L. (2004) Assessing the fit of site-occupancy models. *Journal of Agricultural,*
477 *Biological, and Environmental Statistics*, **9**, 300–318.
- 478 MacKenzie, D. I., Nichols, J. D., Lachman, G. B., Droege, S., Andrew Royle, J. and Langtimm, C. A. (2002)
479 Estimating site occupancy rates when detection probabilities are less than one. *Ecology*, **83**, 2248–2255.
- 480 Fernández-i Marín, X. (2013) Using the ggmcmc package.
- 481 Miller, D. A., Pacifici, K., Sanderlin, J. S. and Reich, B. J. (2019) The recent past and promising future for
482 data integration methods to estimate species' distributions. *Methods in Ecology and Evolution*, **10**, 22–37.
- 483 Morishita, M. (1996) On the influence of the sample size upon the values of species diversity. *Jpn. J. Ecol.*, **46**,
484 269–289.
- 485 Nagendra, H. (2002) Opposite trends in response for the shannon and simpson indices of landscape diversity.
486 *Applied geography*, **22**, 175–186.

- 487 Nicenboim, B., Schad, D. and Vasishth, S. (2021) An introduction to bayesian data analysis for cognitive
488 science. *Under contract with Chapman and Hall/CRC Statistics in the Social and Behavioral Sciences*
489 *Series*.
- 490 O'Connor, R. S., Kunin, W. E., Garratt, M. P., Potts, S. G., Roy, H. E., Andrews, C., Jones, C. M., Peyton, J. M.,
491 Savage, J., Harvey, M. C. et al. (2019) Monitoring insect pollinators and flower visitation: The effectiveness
492 and feasibility of different survey methods. *Methods in Ecology and Evolution*, **10**, 2129–2140.
- 493 O'hara, R. (2005) Species richness estimators: how many species can dance on the head of a pin? *Journal of*
494 *Animal Ecology*, 375–386.
- 495 Ovaskainen, O. and Abrego, N. (2020) *Joint Species Distribution Modelling: Biotic Interactions*, 142–183.
496 Ecology, Biodiversity and Conservation. Cambridge University Press.
- 497 Pacifici, K., Reich, B. J., Miller, D. A., Gardner, B., Stauffer, G., Singh, S., McKerrow, A. and Collazo, J. A.
498 (2017) Integrating multiple data sources in species distribution modeling: a framework for data fusion.
499 *Ecology*, **98**, 840–850.
- 500 Pacifici, K., Reich, B. J., Miller, D. A. and Pease, B. S. (2019) Resolving misaligned spatial data with integrated
501 species distribution models. *Ecology*, **100**, e02709.
- 502 Potts, S., Dauber, J., Hochkirch, A., Oteman, B., Roy, D., Ahrne, K., Biesmeijer, K., Breeze, T., Carvell,
503 C., Ferreira, C. et al. (2020) Proposal for an eu pollinator monitoring scheme. *Publications Office of the*
504 *European Union: Ispra, Italy*.
- 505 Pouteau, R., Bayle, É., Blanchard, É., Birnbaum, P., Cassan, J.-J., Hequet, V., Ibanez, T. and Vandrot, H.
506 (2015) Accounting for the indirect area effect in stacked species distribution models to map species richness
507 in a montane biodiversity hotspot. *Diversity and Distributions*, **21**, 1329–1338.
- 508 R Core Team (2022) *R: A Language and Environment for Statistical Computing*. R Foundation for Statistical
509 Computing, Vienna, Austria. URL: <https://www.R-project.org/>.
- 510 Redko, I., Morvant, E., Habrard, A., Sebban, M. and Bennani, Y. (2019) *Advances in domain adaptation*
511 *theory*. Elsevier.

- 512 Roswell, M., Dushoff, J. and Winfree, R. (2021) A conceptual guide to measuring species diversity. *Oikos*,
513 **130**, 321–338.
- 514 Schaub, M., Gimenez, O., Sierro, A. and Arlettaz, R. (2007) Use of integrated modeling to enhance estimates
515 of population dynamics obtained from limited data. *Conservation Biology*, **21**, 945–955.
- 516 Scheme, U. P. M. (2022a) Flower-insect timed count data from the uk pollinator monitoring scheme, 2017-2020
517 version 2. URL: <https://doi.org/10.5285/13aed7ac-334f-4bb7-b476-4f1c3da45a13>.
- 518 — (2022b) Pan-trap survey data from the uk pollinator monitoring scheme, 2017-2020. URL: <https://doi.org/10.5285/06cc6b8f-9bd4-4ae4-af5d-65bcbd319e9f>.
- 520 Simmonds, E. G., Jarvis, S. G., Henrys, P. A., Isaac, N. J. and O’Hara, R. B. (2020) Is more data always better?
521 a simulation study of benefits and limitations of integrated distribution models. *Ecography*, **43**, 1413–1422.
- 522 Song, Q., Wang, B., Wang, J. and Niu, X. (2016) Endangered and endemic species increase forest conservation
523 values of species diversity based on the shannon-wiener index. *iForest-Biogeosciences and Forestry*, **9**, 469.
- 524 Strebel, N., Kéry, M., Guélat, J. and Sattler, T. (2022) Spatiotemporal modelling of abundance from multiple
525 data sources in an integrated spatial distribution model. *Journal of Biogeography*.
- 526 Team, R. C., Team, M. R. C., Suggests, M. and Matrix, S. (2013) Package “stats.”. *RA Lang. Environment Stat.*
527 *Comput. Vienna, Austria: R Foundation for Statistical Computing*.
- 528 Tikhonov, G., Opedal, Ø. H., Abrego, N., Lehtikoinen, A., de Jonge, M. M., Oksanen, J. and Ovaskainen, O.
529 (2020) Joint species distribution modelling with the r-package hmsc. *Methods in ecology and evolution*, **11**,
530 442–447.
- 531 Tobler, M. W., Kéry, M., Hui, F. K., Guillera-Arroita, G., Knaus, P. and Sattler, T. (2019) Joint species
532 distribution models with species correlations and imperfect detection. *Ecology*, **100**, e02754.
- 533 de Valpine, P., Turek, D., Paciorek, C. J., Anderson-Bergman, C., Lang, D. T. and Bodik, R. (2017) Pro-
534 gramming with models: writing statistical algorithms for general model structures with nimble. *Journal of*
535 *Computational and Graphical Statistics*, **26**, 403–413.

- 536 Vehtari, A., Gelman, A. and Gabry, J. (2017) Practical bayesian model evaluation using leave-one-out cross-
537 validation and waic. *Statistics and computing*, **27**, 1413–1432.
- 538 Wright, W. J., Irvine, K. M. and Rodhouse, T. J. (2016) A goodness-of-fit test for occupancy models with
539 correlated within-season revisits. *Ecology and Evolution*, **6**, 5404–5415.
- 540 Zeleny, D. (2020) Analysis of community ecology data in r. davidzeleny. net.
- 541 Zulian, V., Miller, D. A. and Ferraz, G. (2021) Integrating citizen-science and planned-survey data improves
542 species distribution estimates. *Diversity and Distributions*, **27**, 2498–2509.